

Shape and composition of PMC particles derived from satellite remote sensing measurements

M. N. Eremenko,¹ S. V. Petelina,² A. Y. Zasetsky,¹ B. Karlsson,³ C. P. Rinsland,⁴
E. J. Llewellyn,² and J. J. Sloan¹

Received 16 March 2005; revised 5 May 2005; accepted 18 May 2005; published 28 June 2005.

[1] The Atmospheric Chemistry Experiment Fourier Transform Spectrometer (ACE-FTS) on the SciSat satellite measured nearly 30 spectra of polar mesospheric clouds (PMCs) between 65° and 70°N from July 5 to 14, 2004. The ACE-FTS measurements are augmented by UV observations made at the same latitude and time period by the Optical Spectrograph and Infrared Imager System (OSIRIS) on the Odin satellite. Our analysis of these measurements shows that PMC particles are composed of nonspherical ice crystals with mean (equivalent spherical) particle radii of 59 ± 5 nm. **Citation:** Eremenko, M. N., S. V. Petelina, A. Y. Zasetsky, B. Karlsson, C. P. Rinsland, E. J. Llewellyn, and J. J. Sloan (2005), Shape and composition of PMC particles derived from satellite remote sensing measurements, *Geophys. Res. Lett.*, 32, L16S06, doi:10.1029/2005GL023013.

1. Introduction

[2] High altitude clouds in the polar summer mesosphere have been studied extensively using surface observations as well as rocket and satellite measurements [Thomas and Olivero, 1989]. These clouds usually form above 50° near the summer mesopause (80–85 km) where the atmosphere is sufficiently cold for water ice to exist, and their distribution and particle density may serve as a sensitive indicator of climate change [Gadsden and Schroder, 1989; Thomas et al., 1989]. A detailed description of the history and results of PMC observations are given by Gadsden and Schroder [1989], von Zahn et al. [2004] and DeLand et al. [2003].

[3] Previous work has shown that PMCs consist of particles with radii smaller than about 100 nm [Debrestian et al., 1997; Gumbel and Witt, 1998; Rusch et al., 1991]. Another example of infrared measurements of PMCs is given by Stevens et al. [2003]. The shape of these particles, however, is still not well understood as most of the satellite and ground-based observations of PMCs were made in the UV-VIS and near-IR spectral ranges where ice has no unique absorption features. The first infrared observations of PMCs by the Halogen Occultation Experiment (HALOE) were reported by Hervig et al. [2001] and more recently by

McHugh et al. [2003]. The HALOE PMC measurements at eight wavelengths between 2.4 μm and 9.9 μm with ~ 3 km vertical resolution were in qualitative agreement with model spectra based on ice particle extinction. The limited number of HALOE wavelengths in this region, however, was insufficient to distinguish between extinction by water ice, liquid water and water vapor. The shape of the water extinction spectrum between 2.4 and 9.9 μm is similar to that of ice, with the biggest difference in the region between 2.8 and 3.3 μm , which is not covered by the HALOE measurements. This feature, which proves that the clouds are composed of ice particles, is reported here.

[4] In contrast, the solar occultation spectra recorded by the ACE-FTS instrument [Bernath, 2004] have a broad bandwidth (750–4400 cm^{-1}) and high spectral resolution (0.02 cm^{-1}). Information from spectral bands at several wavelength regions across this bandwidth confirms that the PMC particles are composed of crystalline ice. Moreover, the shape of the band at 3200 cm^{-1} , revealed in detail by the high resolution of the spectra, shows that the particles are not spherical.

[5] Accurate size information for particles smaller than about 100 nm cannot be retrieved from the infrared spectra alone. Therefore, the ACE-FTS PMC measurements are augmented by UV observations of clouds made by the Optical Spectrograph and Infrared Imager System (OSIRIS) on the Odin satellite, which permit the PMC particle sizes to be retrieved. In the following, we report the analysis of PMC observations made by ACE-FTS and Odin/OSIRIS instruments between 65° and 70°N during July 2004.

2. Instrument Description

[6] The SciSat has a circular orbit at 650 km altitude with 74° inclination. The ACE-FTS instrument operates in solar occultation mode with a field of view of 1.25 mrad - about 4 km at the tangent point - and a vertical resolution of 3–4 km from cloud top in the troposphere to about 150 km. The instrumental signal to noise ratio exceeds 100 for single measurements in the spectral region used in this work. Stratospheric and mesospheric temperature and volume mixing ratio profiles of 18 molecular gases have been derived in version 1 FTS processing (C. B. Boone et al., Retrievals for the Atmospheric Chemistry Experiment Fourier Transform Spectrometer, submitted to *Applied Optics*, 2005).

[7] The Odin satellite is a joint Sweden-Canada-France-Finland mission. It has a sun-synchronous, near-terminator orbit with latitudinal coverage in the orbit plane from 82.2°N to 82.2°S [Murtagh et al., 2002]. Odin/OSIRIS scans the Earth limb from 6 to 110 km (strat-meso mode)

¹Departments of Chemistry and Physics, University of Waterloo, Waterloo, Ontario, Canada.

²Department of Physics and Engineering Physics, University of Saskatchewan, Saskatoon, Saskatchewan, Canada.

³Department of Meteorology, Stockholm University, Stockholm, Sweden.

⁴NASA Langley Research Center, Hampton, Virginia, USA.

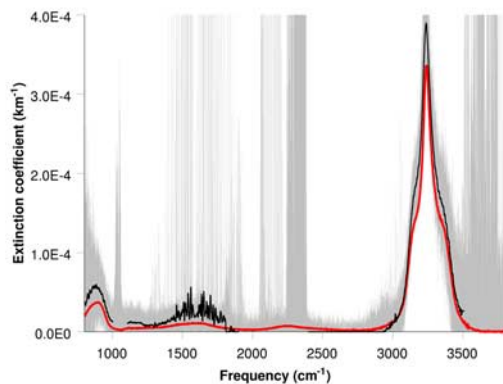


Figure 1. Ten co-added spectra recorded near the polar mesopause in July 2004. Light grey shading: raw spectra; black line: smoothed spectra showing structure of OH vibrational band at 3300 cm^{-1} as well as the librational (800 cm^{-1}) and bending (1600 cm^{-1}) bands; red line: calculated ice aerosol spectrum assuming mean radius of $0.06\text{ }\mu\text{m}$; particle density of 187 cm^{-3} and a path length of 100 km .

or from 60 to 110 km (mesospheric mode) with a vertical speed of $0.75\text{ km per second}$, observing the limb-scattered solar radiance in the spectral range $280\text{--}810\text{ nm}$ with $\sim 1\text{ nm}$ resolution [Llewellyn *et al.*, 2004].

3. ACE-FTS PMC Spectra

[8] During July 5–14, 2004, the SciSat-1 satellite recorded 50 occultations having tangent points between 60°N and 70°N . Signatures of PMC extinctions were observed in 29 of these, while the rest show no evidence of condensed phase extinction at PMC altitudes. The cloud observations were distributed approximately evenly around the pole at apparent tangent altitudes of $75\text{--}85\text{ km}$. Altitudes are approximate because in occultation measurements, clouds not located exactly at the tangent point appear to be at lower altitudes. For example, a cloud at an altitude of 80 km that is 250 km from the tangent point would appear to be at 75 km .

[9] At the altitudes and in the spectral region of interest the influence of gas phase absorption is negligibly small and the signal to noise ratio of the raw spectra is about 5. In processing, the observed spectrum is first smoothed by a wavelet filter to reduce the high frequency noise [Aballe *et al.*, 2001]. The condensed phase retrieval is based on the comparison of the observed spectrum with computed reference spectra of particles having sizes and shapes encompassing the range expected for PMC particles [Zasetsky *et al.*, 2004].

[10] The refractive indices of ice in the temperature range of $130\text{--}210\text{ K}$ [Clapp *et al.*, 1995] were used for all spectrum calculations. The reference extinction spectra of spherical ice particles were calculated using Mie theory [Bohren and Huffman, 1983]. The extinction efficiencies Q of randomly oriented spheroids and cylinders were computed using the T-matrix method of [Mishchenko and Travis, 1998]. Extinction spectra have been calculated for both prolate- and oblate spheroids and cylinders that have aspect ratios in the

range of $0.2\text{--}5.5$. The extinction efficiency of hexagonal prisms was computed using the Discrete Dipole (DD) technique. We also performed calculations for hexagons with length to side ratio between 1 and 2.8 [Pruppacher and Klett, 1998].

[11] For comparison with the observations, the calculated spectra of nonspherical crystals had to be orientationally averaged. Taking advantage of the hexagonal symmetry, a total of 60 orientations were used in the calculations. In the DD calculations, the criterion $2\pi d|n^*|/\lambda < 1$ - where d is the inter-dipole separation, n^* is the complex refractive index, and λ is the wavelength - was satisfied using a total number of dipoles on the order of $10^2\text{--}10^3$. This also ensured that the inter-dipole separation was much smaller than any structural lengths (B. T. Draine and P. J. Flatau, User guide for the Discrete Dipole Approximation Code DDSCAT.6.0, <http://arxiv.org/abs/astro-ph/0309069>, 2003). In the following, when we refer to the sizes of nonspherical particles, we use the radii of spheres having the same volumes.

[12] The grey shaded region in Figure 1 shows the sum obtained by adding 10 of the 29 PMC spectra recorded in this altitude range. The black curve results from smoothing this co-added spectrum. The shape of the OH band in the smoothed spectrum - a sharp central peak with two shoulders - confirms that the particles consist of crystalline ice. The intensity of the PMC spectrum is consistent with the change in the water vapor mixing ratio retrieved using the same group of ACE observations. On average, the difference in the values of water vapor partial pressure between PMC and PMC-free observations is $5.2\text{ }10^8\text{ molecules/cm}^3$. If a mean radius of 60 nm is assumed for the PMC particles (*vide infra*), this would produce an ice particle density of 187 cm^{-3} . The spectrum shown in red in Figure 1 was computed assuming these parameters and choosing a cloud horizontal extent of 100 km . This is in good qualitative agreement with the observed ACE PMC spectra.

[13] Figure 2 shows two observations from a single occultation in the mesospheric region. Figure 2 (top) is in

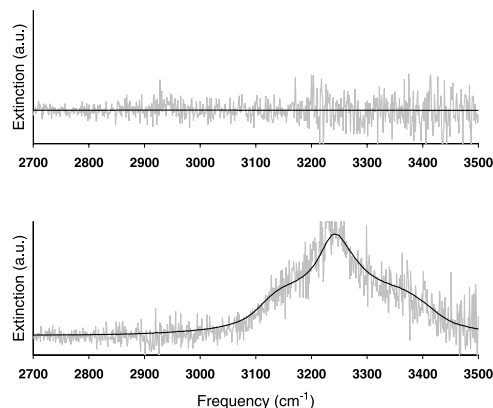


Figure 2. Single spectra recorded near the polar mesopause in July 2004: (top) cloud-free spectrum, (bottom) PMC spectrum, dark line gives the fit obtained using our retrieval method.

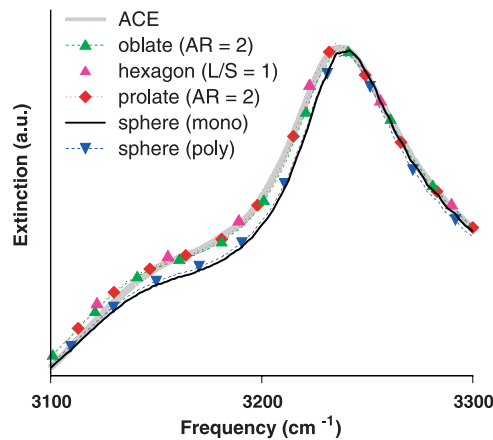


Figure 3. Comparison of the O-H stretch region of the ACE spectrum with extinction spectra computed using different particle shapes. The optical constants of [Clapp *et al.*, 1995] for a temperature of 130 K were used in the computations.

a cloud-free region at 88 km just above the PMC and Figure 2 (bottom) is at the peak of the PMC density at 82 km.

4. PMC Particle Shapes Derived From Infrared Spectra

[14] Information about the PMC particle shape can be obtained from the cloud spectra because the shape affects the structure of the O-H band. This is illustrated in Figure 3 where the light grey curve marked “ACE” is a section of the co-added spectrum shown in Figure 1. The solid black curve shows monodisperse spherical particles with a radius of 60 nm. Falling nearly on top of this (downward pointing triangles) is the spectrum of a sample of spheres with a uniform distribution of radii between 20 and 100 nm, labelled “polydisperse.” The measured spectrum agrees with these computed spherical spectra on the high frequency side of the band, but deviates significantly on the low frequency side between about 3100 cm^{-1} and 3250 cm^{-1} .

[15] The spectra of monodisperse and polydisperse spheres are nearly identical and the shape of the O-H band is invariant with size in this size range. This proves that effects such as morphology dependent resonances are not responsible for the observed deviations in the band shape, because these occur with monodisperse samples and disappear for even narrow polydisperse size distributions. Moreover, neither spectrum agrees with the ACE observations. Thus we can conclude that the PMC particles are not spherical.

[16] A plausible explanation for the deviations between the observed and calculated spectra is based on resonant effects (or surface modes) in spherical particles. The effects are known to affect absorption band shapes [Mishchenko, 1991] and are considerable for very small particles, the absorption features of which are dominated by shape in the case of samples with high absorption [Bohren and Huffman, 1983]. In the extinction spectra of ice nanoparticles in the O-H absorption region, the surface modes for ideal spheres result in a narrow, symmetric band centred near 3235 cm^{-1} .

[17] The spectra of randomly oriented aspherical particles reproduce the ACE spectra much better than the spectra of

spheres. We found that both oblate and prolate spheroids with aspect ratios of about 2, as well as hexagons with length-to-side ratios near 1 are equally good at reproducing the experimental band shape. The spectra of these three shapes are also shown in Figure 3 for particles with an equivalent radius of 60 nm. In all three cases, the computed spectra of nonspherical particles are indistinguishable from the ACE observation. Spectra that are very similar to the ACE observations are also seen in the rapid expansion of water vapour in helium [Devlin *et al.*, 2001]. The similarity between these lab spectra and the ACE observations is additional support for the claim that the band shapes in the latter are not caused by instrumental effects.

[18] We are continuing to investigate the band shapes of the recorded spectra, with the assistance of laboratory and computational studies [Buch *et al.*, 2004], to derive further information about the microphysical properties of the particles.

5. Particle Sizes Derived From Odin/OSIRIS Observations

[19] As noted previously, it is generally agreed that PMC particle radii are in the range of 10 to 100 nm [Baumgarten *et al.*, 2002; Carbary *et al.*, 2002; Debrestian *et al.*, 1997; Gumbel and Witt, 1998; Rusch *et al.*, 1991]. Infrared measurements by the ACE-FTS cannot give size information directly for particles smaller than about 100 nm, so we are not able to determine precise particle sizes by simple inversion of the IR spectra. From the infrared spectrum shown in Figure 1 we can conclude only that the particles are smaller than 100 nm. Also, the sharp central peak in the O-H stretch region implies that the particles are larger than 10 nm [Devlin *et al.*, 2001]. The Odin/OSIRIS measurements, however, give much more precise size information.

[20] The enhanced radiance in the mesospheric region is a well-established signature that has been used to detect PMCs from satellite limb observations [Olivero and Thomas, 1986; Thomas and Olivero, 1989]. The Odin/OSIRIS PMC detection method is based on the ratio of the measured scattered radiance to the corresponding Rayleigh background between 80 km and 88 km. This ratio, termed the relative brightness (RB), is equal to unity when no PMC is present. Further details on OSIRIS PMC detections and PMC database are given by Petelina *et al.* [2005].

[21] A typical example of OSIRIS PMC-containing limb radiance profiles and a map of the Odin mesospheric coverage and OSIRIS PMC detections during 24 hours of measurements are shown in Figures 4a and 4b, respectively. We note that while most of the bright clouds with $\text{RB} > 10$ were observed by OSIRIS poleward of 70N, about 1 to 5 bright clouds per day were detected in the same latitude region as the ACE PMCs.

[22] We have estimated the particle sizes for each of the OSIRIS bright clouds ($\text{RB} \geq 10$) measured during July 2–14, 2004, between 65° and 70°N . The analysis is performed in the 280–305 nm spectral range using a method similar to that described by von Savigny *et al.* [2005] except for the assumption of a monodisperse size distribution instead of the lognormal one employed in the referenced paper. By comparing individual OSIRIS PMC spectra with Mie calculations of the spectra of homogeneous ice spheres, we retrieved a mean effective radius of 59 nm, with standard

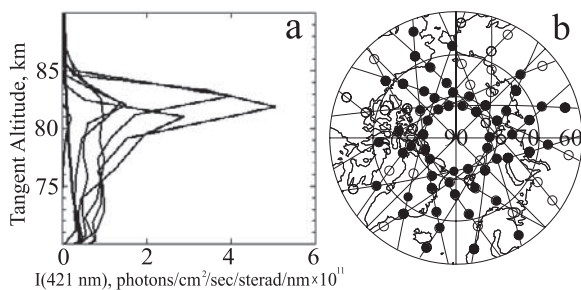


Figure 4. (a) Typical PMC-containing limb radiance profiles at 421 nm, with the Rayleigh background removed, measured during a single orbit on July 6, 2004. (b) Example of the Odin/OSIRIS daily mesospheric coverage poleward of 60°N and the corresponding PMC detections. Solid lines – ground projections of the Odin/OSIRIS line of sight tangent point; transparent circles – locations where Odin/OSIRIS could have seen a PMC but did not; filled circles – locations where Odin/OSIRIS detected a PMC.

deviation of 5 nm. As shown by Baumgarten *et al.* [2002], the shape of cloud particles can be estimated from polarization measurements, but not from the lidar backscatter ratio in the UV-VIS. Similarly, OSIRIS UV-VIS measurements are not sensitive to particle shapes, and the Mie spheres approximation can be used for particle size retrievals.

[23] We note that the direct comparison of individual ACE and OSIRIS PMC observations is not possible because PMCs consist of highly inhomogeneous layers with smaller structures of the order of 1–10 km and temporal variability below 1 hour. As a result, the measurements of the same PMC field from different satellites may produce different cloud properties due to the differences in the small-scale structures along the line-of-sight.

6. Conclusions

[24] We have reported the observation of several PMCs during July of 2004 by instruments on the SciSat and Odin satellites. The measurements were done by solar occultation in the infrared and limb scattering in the UV. By combining the observations, we have identified these clouds unequivocally as nonspherical ice crystals in the size range 59 ± 5 nm.

[25] **Acknowledgments.** The authors thank Victoria Buch, Paul Devlin and Michael Mishchenko for helpful discussions; Georg Witt for discussions on PMCs and the ACE team for assistance with access to the ACE database. We acknowledge financial support from the Canadian Space Agency (CSA) and the Natural Sciences and Engineering Research Council of Canada. Odin is a Swedish-led satellite project funded jointly by Sweden (SNSB), Canada (CSA), France (CNES) and Finland (Tekes). SciSat is funded by the CSA.

References

Aballe, A. M., *et al.* (2001), Use of wavelets to study electrochemical noise transients, *Electrochim. Acta*, *46*, 2353–2361.
 Baumgarten, G., K. H. Fricke, and G. von Cossart (2002), Investigation of the shape of noctilucent cloud particles by polarization lidar technique, *Geophys. Res. Lett.*, *29*(13), 1630, doi:10.1029/2001GL013877.
 Bernath, P. F. (2004), Atmospheric chemistry experiment (ACE): Mission overview, *Proc. SPIE Int. Soc. Opt. Eng.*, *5542*, 146–156.

Bohren, G., and D. Huffman (1983), *Absorption and Scattering of Light by Small Particles*, John Wiley, Hoboken, N. J.
 Buch, V., *et al.* (2004), Solid water clusters in the size range of tens-thousands of H₂O: A combined computational/spectroscopic outlook, *Int. Rev. Phys. Chem.*, *23*, 375–433.
 Carbarry, J. F., D. Morrison, and G. J. Romick (2002), Particle characteristics from the spectra of polar mesospheric clouds, *J. Geophys. Res.*, *107*(D23), 4686, doi:10.1029/2001JD001154.
 Clapp, M. L., *et al.* (1995), Frequency-dependent optical-constants of water ice obtained directly from aerosol extinction spectra, *J. Phys. Chem.*, *99*, 6317–6326.
 Debrestian, D. G., *et al.* (1997), An analysis of POAM II solar occultation observations of polar mesospheric clouds in the southern hemisphere, *J. Geophys. Res.*, *102*, 1971–1981.
 DeLand, M. T., *et al.* (2003), Solar backscattered ultraviolet (SBUV) observations of polar mesospheric clouds (PMCs) over two solar cycles, *J. Geophys. Res.*, *108*(D8), 8445, doi:10.1029/2002JD002398.
 Devlin, J. P., *et al.* (2001), Infrared spectra of large H₂O clusters: New understanding of the elusive bending mode of ice, *J. Phys. Chem. A*, *105*, 974–983.
 Gadsden, M., and W. Schroder (1989), *Noctilucent Clouds*, 165 pp., Springer, New York.
 Gumbel, J., and G. Witt (1998), In situ measurements of the vertical structure of a noctilucent cloud, *Geophys. Res. Lett.*, *25*, 493–496.
 Hervig, M., *et al.* (2001), First confirmation that water ice is the primary component of polar mesospheric clouds, *Geophys. Res. Lett.*, *28*, 971–974.
 Llewellyn, E. G., *et al.* (2004), The OSIRIS instrument on the Odin spacecraft, *Can. J. Phys.*, *82*, 411–422.
 McHugh, M., *et al.* (2003), Improved mesospheric temperature, water vapor and polar mesospheric cloud extinctions from HALOE, *Geophys. Res. Lett.*, *30*(8), 1440, doi:10.1029/2002GL016859.
 Mishchenko, M. I. (1991), Infrared-absorption by shape distributions of NH₃ ice particles—An application to the Jovian atmosphere, *Earth Moon Planets*, *53*, 149–156.
 Mishchenko, M. I., and L. D. Travis (1998), Capabilities and limitations of a current FORTRAN implementation of the T-matrix method for randomly oriented, rotationally symmetric scatterers, *J. Quant. Spectrosc. Radiat. Transfer*, *60*, 309–324.
 Murtagh, D. P., *et al.* (2002), An overview of the Odin atmospheric mission, *Can. J. Phys.*, *80*, 309–319.
 Olivero, J. J., and G. E. Thomas (1986), Climatology of polar mesospheric clouds, *J. Atmos. Sci.*, *43*, 1263–1274.
 Petelina, S. V., *et al.* (2005), Odin/OSIRIS limb observations of polar mesospheric clouds in 2001–2003, *J. Atmos. Solar-Terr. Phys.*, in press.
 Pruppacher, H. R., and J. D. Klett (1998), *Microphysics of Clouds and Precipitation*, Springer, New York.
 Rusch, D. W., G. E. Thomas, and E. J. Jensen (1991), Particle-size distributions in polar mesospheric clouds derived from solar mesosphere explorer measurements, *J. Geophys. Res.*, *96*, 12,933–12,939.
 Stevens, M. H., J. Gumbel, C. R. Englert, K. U. Grossmann, M. Rapp, and P. Hartogh (2003), Polar mesospheric clouds formed from space shuttle exhaust, *Geophys. Res. Lett.*, *30*(10), 1546, doi:10.1029/2003GL017249.
 Thomas, G. E., and J. J. Olivero (1989), Climatology of polar mesospheric clouds: 2. Further analysis of solar mesosphere explorer data, *J. Geophys. Res.*, *94*, 14,673–14,681.
 Thomas, G. E., *et al.* (1989), Relation between increasing methane and the presence of ice clouds at the mesopause, *Nature*, *338*, 490–492.
 von Savigny, C., *et al.* (2005), Vertical variation of NLC particle sizes retrieved from Odin/OSIRIS limb scattering observations, *Geophys. Res. Lett.*, *32*, L07806, doi:10.1029/2004GL021982.
 von Zahn, U., *et al.* (2004), Noctilucent clouds and mesospheric water vapor: The past decade, *Atmos. Chem. Phys.*, *4*, 2449–2464.
 Zaslavsky, A. Y., *et al.* (2004), Characterization of atmospheric aerosols from infrared measurements: Simulations, testing, and applications, *Appl. Opt.*, *43*, 5503–5511.

M. N. Eremenko, J. J. Sloan, and A. Y. Zaslavsky, Departments of Chemistry and Physics, University of Waterloo, Waterloo, ON, Canada N2L 3G1. (sloanj@uwaterloo.ca)

B. Karlsson, Department of Meteorology, Stockholm University, SE-10691 Stockholm, Sweden.

E. Llewellyn and S. V. Petelina, Department of Physics and Engineering Physics, University of Saskatchewan, Saskatoon, SK, Canada S7N 5E2.

C. P. Rinsland, NASA Langley Research Center, Hampton, VA 23681–2199, USA.